pubs.acs.org/acschemicalbiology

Articles

Analysis of the Sequence Preference of Saporin by Deep Sequencing

Samuel Hauf, Rachapun Rotrattanadumrong, and Yohei Yokobayashi*

Cite This: *ACS Chem. Biol.* 2022, 17, 2619–2630

Read Online

ACCESS | Metrics & More | Article Recommendations | Supporting Information

ABSTRACT: Ribosome-inactivating proteins (RIPs) are RNA:adenosine glycosidases that inactivate eukaryotic ribosomes by depurinating the sarcin-ricin loop (SRL) in 28S rRNA. The GAGA sequence at the top of the SRL or at the top of a hairpin loop is assumed to be their target motif. Saporin is a RIP widely used to develop immunotoxins for research and medical applications, but its sequence specificity has not been investigated. Here, we combine the conventional aniline cleavage assay for depurinated nucleic acids with high-throughput sequencing to study sequence-specific depurination of oligonucleotides caused by saporin. Our data reveal the sequence preference of saporin for different substrates and show that the GAGA motif is not efficiently targeted by this protein, neither in RNA nor in DNA. Instead, a preference of saporin for certain hairpin DNAs was observed. The observed sequence-specific activity of saporin may be relevant to antiviral or apoptosis-inducing effects of RIPs. The developed method could also be useful for studying the sequence specificity of depurination by other RIPs or enzymes.

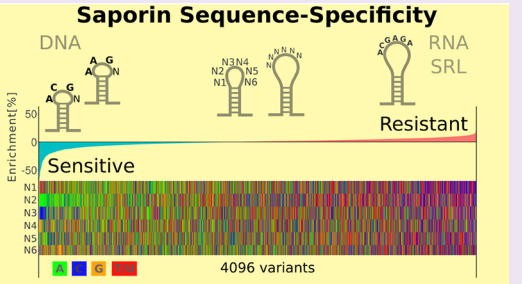

INTRODUCTION

RNA:adenosine glycosidase activity is thought to be the defining feature of all ribosome-inactivating proteins (RIPs).[1] This activity targets the sarcin-ricin loop (SRL), a highly conserved, compact structure of rRNA (rRNA) that is important for the function of ribosomes.[2] RIPs cleave off one adenine base at the top of the SRL.[3] The loss of this adenine base inhibits translocation and inactivates the ribosome.[4] Some RIPs, for example, Shiga toxin and ricin, have been shown to specifically interact with ribosomal stalk proteins to gain access to the SRL.[5,6] This interaction is essential for specificity toward the intact ribosomes and accelerates the depurination reaction,[7] enabling ricin to inactivate approximately 1500 ribosomes per minute in vitro.[8]

Experiments with ricin indicated that a hairpin loop with the GAGA sequence at the top is the minimal element required for RIP activity.[7,9] It has also been shown that RIPs can release adenine from a range of different substrates, such as mRNA or DNA.[10,11] Until now, it has been unclear if and how the specificity of RIPs on other substrates differs from the specificity for ribosomes or rRNA. Saporin, a type I ribosome-inactivating protein produced by the plant *Saponaria officinalis*, was particularly effective at liberating adenine from a range of different nucleic acid species.[12] Compared to ricin that is highly specific for ribosomes, saporin is much more promiscuous and can target oligonucleotides without the aid of other (protein) factors. Thus far, it is unknown if the activity on substrates other than rRNA is also influenced by the sequence of the nucleic acid substrates.

RIPs are generally classified into type I or II depending on their composition. Type I RIPs consist of one protein domain (the A chain) that is catalytically active, while type II RIPs consist of the A chain and a lectin-like domain (the B chain) that can mediate binding and uptake into eukaryotic cells.[1] While type II RIPs (like ricin and Shiga toxin) are usually highly toxic, type I RIPs like saporin are basically nontoxic to humans and can be found in many plants widely consumed as food.[13] The uptake of RIPs by eukaryotic cells is a major determinant of their toxicity.[14] RIP toxicity thus depends on the presence of a specific receptor on the cell surface.[15] RIPs coupled to cancer cell-specific antibodies (so-called immunotoxins) have therefore been investigated for cancer-targeting therapies. Saporin immunotoxins in particular have shown promise for the treatment of cancer or as a conditioning agent for the treatment of immune malfunction due to RAG deficiency.[16−19] Saporin-based immunotoxins have also been used to kill specific types of neurons and to study their effect on the brain.[20,21] Still, only a few immunotoxins have been approved for treatment because of serious side effects and immunogenicity.[22] Gaining a better understanding of the catalytic activities of saporin might thus aid in the development

Received: June 27, 2022
Accepted: July 29, 2022
Published: August 15, 2022

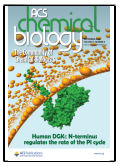

https://doi.org/10.1021/acschembio.2c00531
ACS Chem. Biol. 2022, 17, 2619−2630

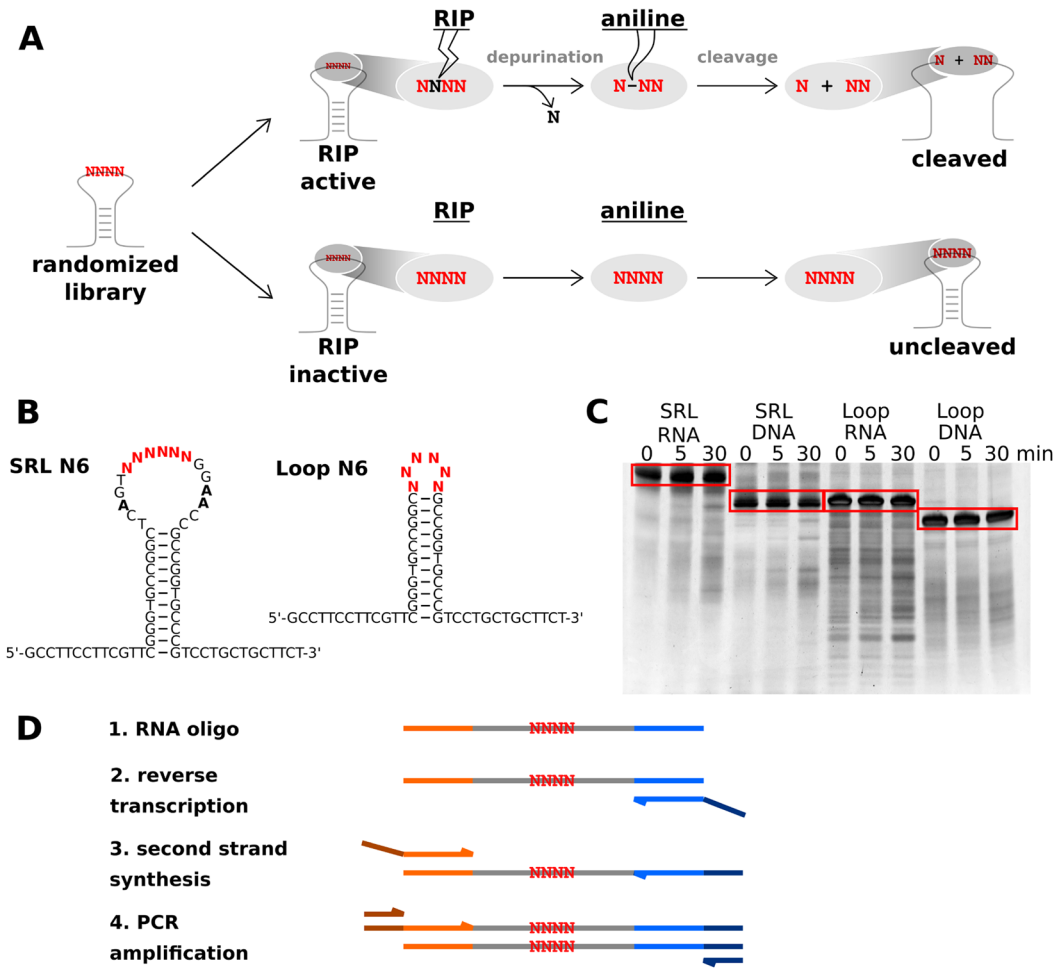

Figure 1. Schematic illustration of the process used to treat the DNA and RNA oligos and to construct sequencing libraries. (A) The randomized library may contain sequences that are susceptible or not susceptible to depurination by the RIP being studied. After RIP treatment, some sequences are depurinated (top). These can be cleaved by aniline at the abasic site. Sequences that are resistant to depurination remain intact (bottom). (B) Sequences and secondary structure of both DNA libraries with six randomized bases (N) in the loop. One was based on the ribosomal rRNA sequence of the SRL with the top ACGAGA sequence randomized. The second contained only the six randomized bases in the loop. Both have a stable 11 bp stem and additional flanking 5′ and 3′ constant regions for reverse transcription and PCR. (C) Uncleaved fragments (boxed in red) can be recovered from a denaturing polyacrylamide gel after different treatment times. (D) RNA oligos were reverse transcribed with a primer annealed to the 3′ end (blue). The second strand of cDNA was synthesized with a primer annealed to the other end of the SRL RNA (orange). The cDNA was amplified in a PCR using Illumina UDI primers annealed to sequence newly added in the previous two steps (dark orange and dark blue), yielding the final sequencing library.

of targeted therapies and the understanding of the side effects of saporin-containing immunotoxins.

High-throughput or deep sequencing is a versatile approach for characterizing the effects enzymes have on nucleic acids. This approach has been used to characterize the sequence specificity of C5, the RNA binding subunit of *Escherichia coli* RNase P, and its RNA processing kinetics.[23] The detailed affinity distributions that could be obtained by sequencing make it possible to gain a much more comprehensive picture of the protein's intrinsic activity.[24] To the best of our knowledge, no such studies have been performed for any RIP.

Here, we present a high-throughput, DNA sequencing-based approach to study the depurination activity of saporin against different nucleic acids. While most RIPs work efficiently on intact ribosomes, our method combines synthetic oligonucleotides with a central randomized region, depurination with saporin, the aniline cleavage assay for depurinated nucleic acids, and high-throughput sequencing. Due to the minimal requirements of this method, it can be easily adapted to study depurination of promiscuous as well as more specific enzymes.

Using this approach, the sequence preference of saporin for DNA and RNA sequences containing six randomized positions was determined. Surprisingly, the wild-type SRL sequence in isolation is not an efficient target for saporin. Instead, small hairpin DNAs containing the motif ACG at the beginning of the loop were found to be most susceptible to depurination. The results from sequencing could be reproduced for selected oligos using the conventional aniline cleavage assay and visualization by polyacrylamide gel electrophoresis (PAGE), showing that saporin preferentially targets these hairpin DNAs. We believe that our method can also be used to determine the sequence preference of other depurinating proteins, for example, the important RIP toxins ricin, abrin, and Shiga toxin. The results presented here might also help other groups with the design of RIP-based immunotoxins, RIP inhibitors,

https://doi.org/10.1021/acschembio.2c00531
ACS Chem. Biol. 2022, 17, 2619−2630

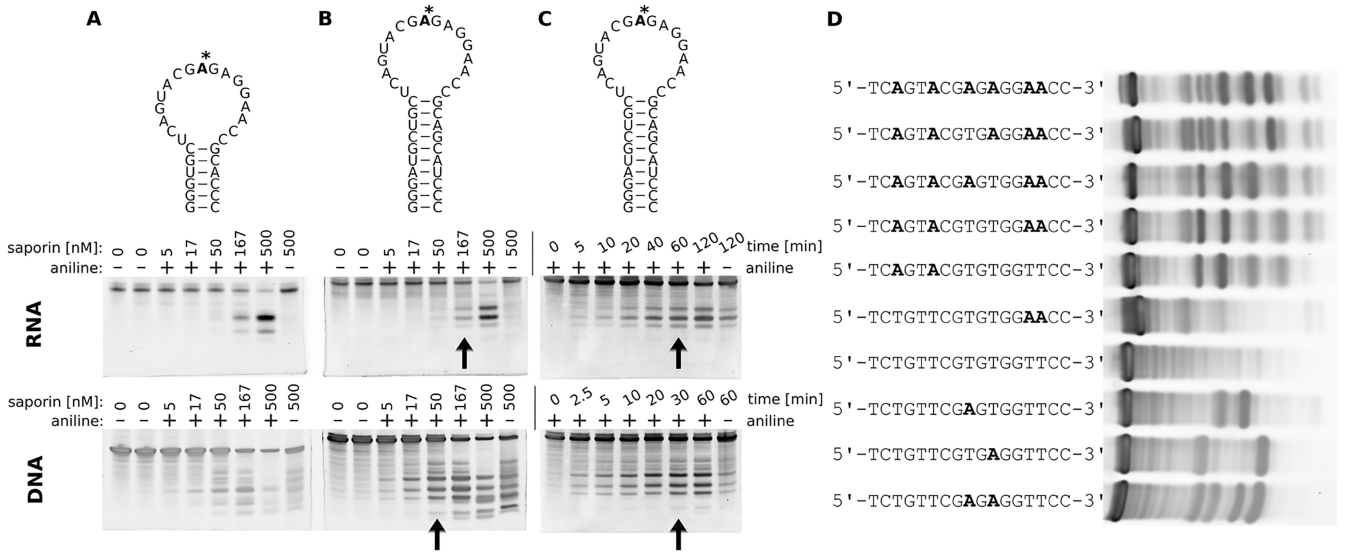

Figure 2. Determination of saporin treatment conditions. (A) Cleavage of RNA (OSaH151) and DNA (OSaH152) variants of E73 after treatment with different amounts of saporin for 30 min. The saporin concentrations were 0, 5, 17, 50, 167, and 500 nM. The last two lanes were both incubated with 500 nM saporin, but aniline treatment was omitted in the last lane. The sequence of the RNA oligo is shown on the top with the targeted adenine marked with an asterisk. (B) Similar to panel A, but using oligos with a more stable (longer) stem (OSaH229 and OSaH190). Arrows indicate the condition chosen for kinetic experiments in panel C. (C) The oligos were treated with the amount of saporin indicated by the arrow in panel B for different lengths of time. The arrows indicate the time points deemed appropriate for sequencing. At these points, cleavage bands are visible, but the bulk of the oligo is still unreacted. (D) Nonspecific depurination of 600 nM DNA oligos (OSaH190, -195, -196, -201, -244, -243, -199, and -207−209 from top to bottom, respectively) by 150 nM saporin. All adenine residues in the wild-type SRL sequence (top) are depurinated to some extent. The GAGA pattern is not required for depurination. In panels A−C, canonical and noncanonical base pairs found in the native SRL sequence are not depicted.

and sensors or help explain RIP antiviral activity and their roles in nature.

RESULTS

Method Overview. Our method uses synthetic DNA oligos with a central randomized region. The sequences selected for the study are based on structures known to be targeted by RIPs such as the SRL[25] or short hairpin loop structures[9] (Figure 1B). For the SRL, the "ACGAGA" sequence at the top of the loop was replaced by six random nucleotides (N) shown in red. The resulting molecules still contain the rest of the original loop, including three conserved adenine residues (bold). Because RIPs act specifically on adenine, the randomized region spanned three adenine bases and no additional adenine residues were included in the stem or the flanking sequences. The short hairpin loop oligos do not contain any adenine residues outside of the randomized region. The DNA oligos are transcribed into RNA using T7 RNA polymerase before treatment with saporin. Alternatively, the DNA oligos are directly incubated with saporin to induce depurination. The resulting abasic sites are cleaved by aniline under acidic conditions[26] (Figure 1A). This step separates the constant regions at the 5′ and 3′ ends of the oligo. The libraries are then loaded on a denaturing polyacrylamide gel to separate cleaved and uncleaved fragments. The uncleaved fragments (Figure 1C, boxed in red) are extracted from the gel and processed into sequencing libraries. The gel picture of the second replicate is shown in Figure S5. The constant regions of the oligos are used to anneal primers for reverse transcription and second-strand synthesis. The primers used also introduce the sequencing adapters necessary for Illumina sequencing (Figure 1D). A final polymerase chain reaction (PCR) using Illumina UDI primers is performed to amplify the library. The number of PCR cycles was optimized to minimize PCR-introduced bias. The use of unique molecular identifiers (UMIs) could further reduce such bias if more precise quantification is desired.[27] To find the sequences that are depurinated and cleaved, the abundance of sequence variants in a library before and after saporin treatment (here, 0 min meaning immediate quenching and 30 min treatment) is compared.

Depurination Activity of Saporin on SRL-Based DNA and RNA Substrates. We began our study by determining the conditions necessary to achieve measurable depurination and cleavage of RNA and DNA substrates with saporin using the conventional aniline cleavage assay. For this purpose, we initially chose E73,[25] an oligo mimic of the SRL, as the substrate. DNA and RNA versions of this sequence were generated by solid phase synthesis and treated with different amounts of saporin using a published protocol.[3] The resulting abasic sites were cleaved by aniline, and the oligos were loaded onto a denaturing polyacrylamide gel. The RNA yielded cleavage bands whose appearance strictly depended on aniline cleavage (Figure 2A). For DNA, faint cleavage bands were also observed without aniline treatment. These are most likely the result of spontaneous hydrolysis at the abasic site, because compared to abasic RNA, abasic DNA is very unstable.[26]

Interestingly, DNA seemed to be more sensitive to depurination by saporin than RNA. Visible cleavage bands were observed after treatment with 500 fmol (17 nM) of saporin, while 5 pmol (167 nM) of saporin was required for the RNA substrate (Figure 2A). Similar findings have already been reported for other RIPs. For example, the ricin A chain had higher activity on short linear DNA oligos than on RNA

https://doi.org/10.1021/acschembio.2c00531
ACS Chem. Biol. 2022, 17, 2619−2630

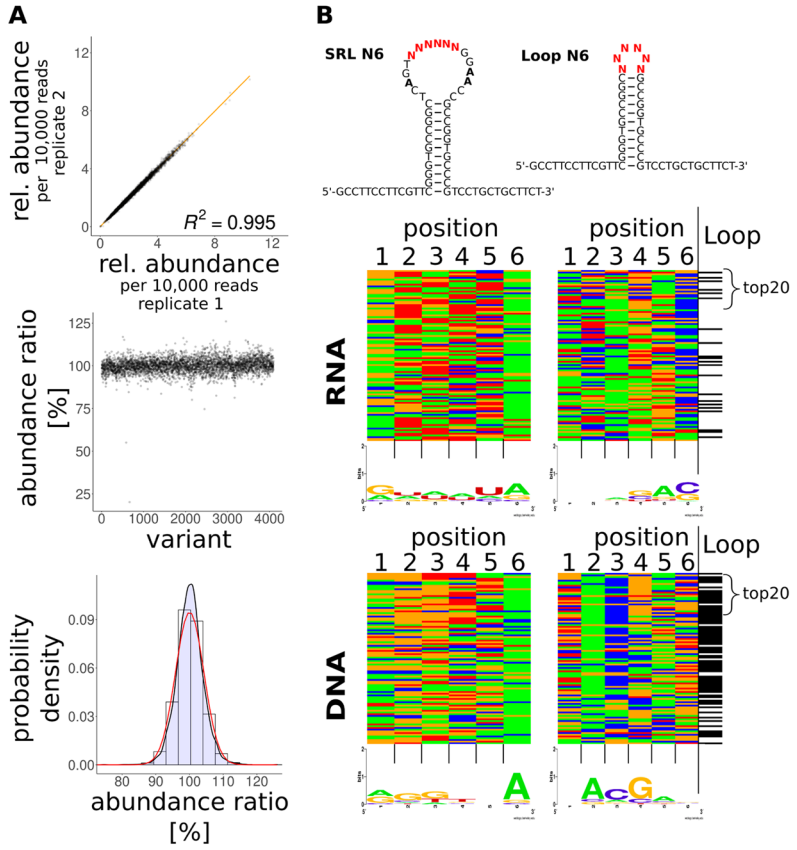

Figure 3. Results of the saporin substrate sequencing assays. (A) Two independent treatments of the libraries with saporin were highly reproducible. All variants correlated linearly as shown for the DNA loop library. Judging from the scatter and histogram plots of the abundance ratio across both replicates, the error caused by the method is randomly distributed. The density of the data (blue) closely follows that of a normal distribution (red). (B) Sequence representation of the 100 most efficiently depurinated variants from each library with a sequence logo based on the top 20 variants. Bases are colored green for A, blue for C, orange for G, and red for T (or U). The last column, which is present for only the loop libraries, indicates the possibility of base pairing between randomized positions 1 and 6. Complementary bases at these positions are colored black, while mismatched bases are colored white.

variants[10] and Shiga toxin has also been found to be highly active on DNA.[28]

If the E73 oligos were depurinated and cleaved at the first A in the GAGA motif, cleavage should yield two fragments of identical size. Instead, our experiment yielded two fragments for the RNA oligo and one intense band as well as some fainter bands for the DNA oligo. We assumed that the short (6 bp) stem of E73 might not be stable and allows different structures to form. These might be depurinated at different sites. Therefore, new oligos that had a more stable 10 bp stem with the same loop region as E73 were designed and treated with saporin under the same conditions. Native PAGE was performed to confirm that, under the experimental conditions, the oligos used do not form dimers that disrupt the stem−loop structure (Figure S1). The new versions of E73 also did not yield the expected cleavage pattern of two fragments with nearly identical sizes (Figure 2B). Instead, three intense bands and some fainter bands were observed, especially for the DNA oligo (Figure 2B). To test the effect of single adenine bases on the cleavage pattern of the DNA oligo, all adenine bases in the loop region were mutated to thymidine.

Nonspecific DNA:Adenosine Glycosidase Activity. Figure 2D shows the cleavage bands observed for variants of SRL-based DNA substrates. The results indicate that the GAGA sequence is not required for depurination. All adenine residues seem to be targeted by saporin at the concentration used (150 nM saporin and 600 nM DNA), although the adenines at the 3′ end of the loop are depurinated less efficiently. As expected, a substrate without adenine in the loop region was not depurinated and therefore not cleaved by aniline. The introduction of a single adenine residue was enough for cleavage bands to appear. A control experiment showing untreated oligos can be found in Figure S2. Interestingly, adenine residues in the stem of these oligos did not seem to contribute to the cleavage pattern. These residues form Watson−Crick base pairs and are most likely not accessible to saporin. Saporin thus seems to be a nonspecific single-strand polynucleotide:adenosine glycosidase. This is in contrast to results obtained with ricin, which seems to be more specific, at least for RNA oligos.[9,10]

Optimizing the Reaction Time for Depurination. Using the minimal saporin concentrations necessary to induce significant cleavage of the SRL mimic (Figure 2B, indicated by the arrows), we next performed depurination kinetic experiments to estimate the time required for optimal cleavage using the same aniline cleavage assay. Fifteen picomoles (500 nM) of the SRL mimic was treated with 5 pmol (167 nM) of saporin in the case of RNA and 1.5 pmol (50 nM) of saporin in the case of DNA. According to the results, we decided to treat the RNA libraries for 60 min and the DNA libraries for 30 min

https://doi.org/10.1021/acschembio.2c00531
ACS Chem. Biol. 2022, 17, 2619−2630

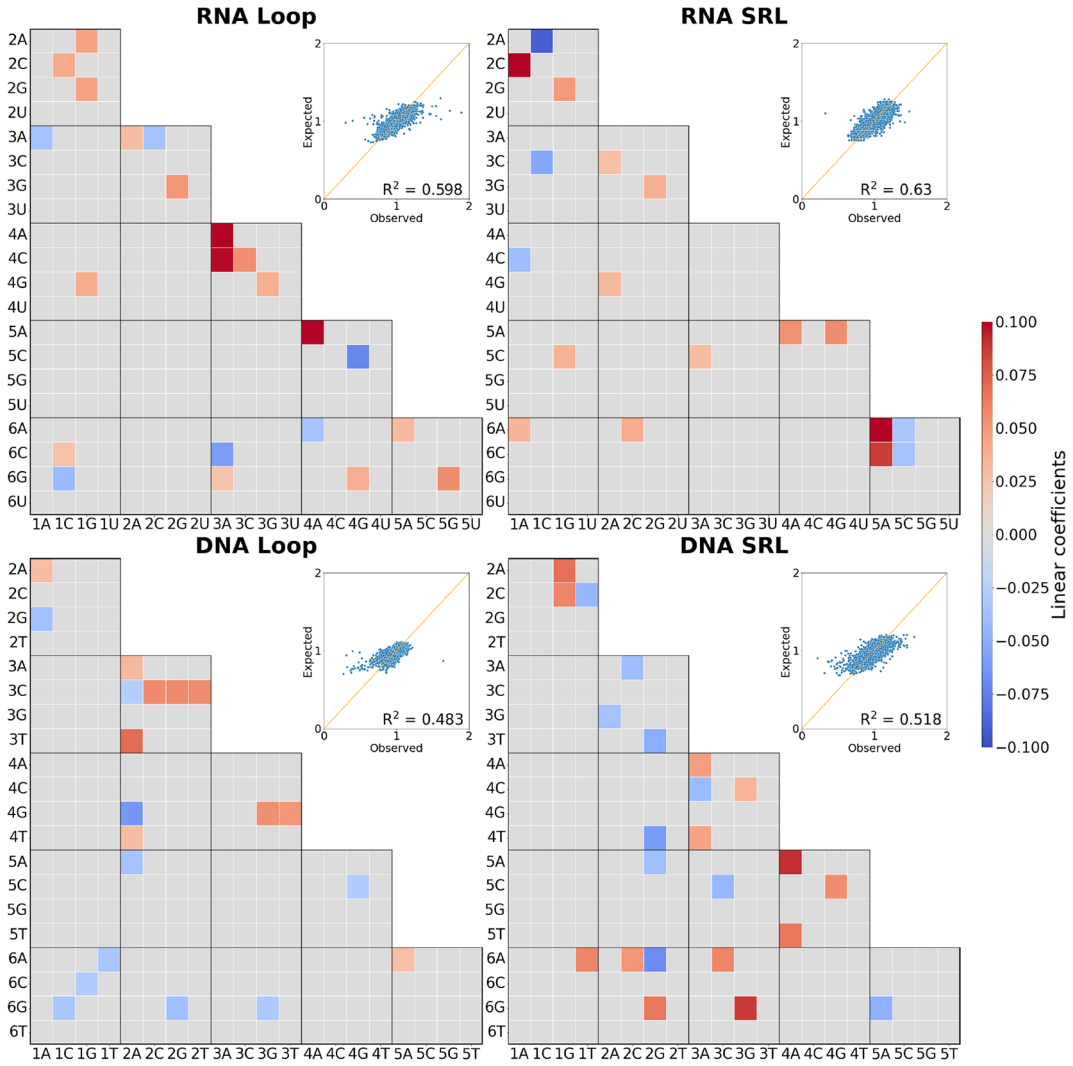

Figure 4. Matrices for the pairwise coupling model. The recovery ratio was used to fit linear regression models that consider pairwise interactions between bases at different positions (see Materials and Methods). The insets show the R^2 values (coefficients of determination) between the predicted and observed recovery ratios for each model. Each square shows the linear coefficients of the model that indicate how a particular pair of base combination affects model prediction of the recovery ratio. Blue squares (low linear coefficient) indicate that this base combination promotes depurination by saporin, while red fields (high linear coefficient) indicate that the base combination inhibits depurination. Gray squares show pairs of bases that do not significantly affect depurination by saporin.

(Figure 2C, indicated by the arrows). At this time point, there should be measurable cleavage because cleavage bands were clearly visible while most of the oligo (around 80%) was still uncleaved. If the reaction were to proceed too far, it would not be possible to differentiate the sequences with strong to moderate substrate preferences.

While treating the randomized libraries with saporin using the conditions determined so far, we found that the DNA library behaved as expected but the RNA library was cleaved more than expected (data not shown). This suggested that the RNA form of the SRL mimic might be more resistant to saporin depurination than most variants in the randomized library. Therefore, we decided to treat the RNA library using the same conditions as determined for DNA [15 pmol (500 nM) of library with 1.5 pmol (50 nM) of saporin for 0 and 30 min]. In this case, we could indeed observe cleavage bands for the randomized RNA and DNA libraries, while the bulk of each library was still uncleaved after 30 min at 37 °C. The uncleaved fractions were purified from a polyacrylamide gel (Figure 1C) and processed for sequencing. The conditions established thus far (50 nM saporin, 500 nM library, 30 min, and 37 °C) are likely substrate limiting. With 4096 total variants in a library, the concentration of each variant averages 122 pM, which is substantially lower than the previously reported K_M values for SRL-based substrates targeted by saporin (9−95 μM).[29,30]

Reproducibility of the Sequencing Assay. We performed two independent saporin treatments of the randomized libraries to evaluate the reproducibility of the method. The relative abundance (count of one variant divided by the sum of the counts of all of the variants) of each variant in the library is highly reproducible even after saporin treatment (Figure 3A, top, and Figure S3). The method-induced error was estimated by comparing the ratio of the relative abundance for each variant in replicates 1 and 2, termed the "abundance ratio". As expected, across the replicates, the abundance ratio is near 100% and the error seems (except for some outliers) to be randomly distributed

https://doi.org/10.1021/acschembio.2c00531
ACS Chem. Biol. 2022, 17, 2619−2630

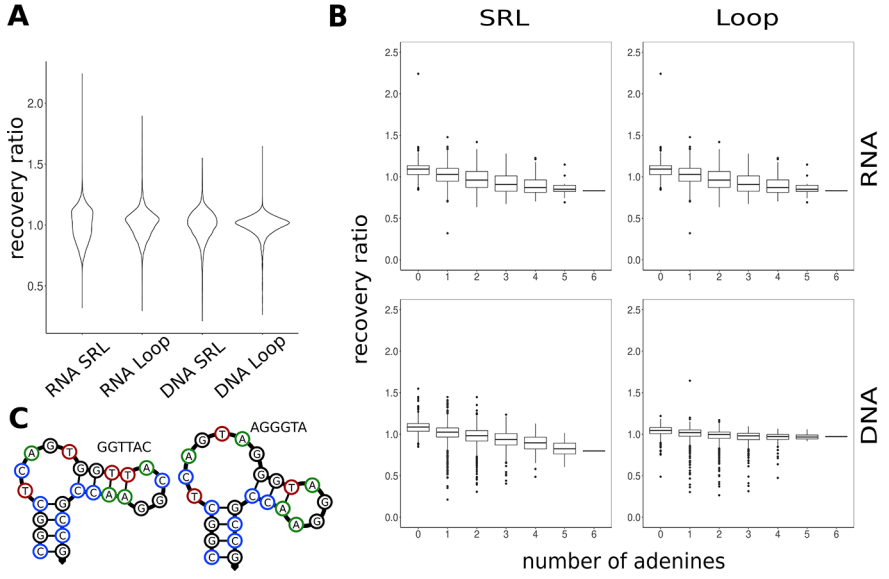

Figure 5. Distribution of recovery ratios. (A) Shape of the distribution of recovery ratios for all variants. The distributions of the SRL-based libraries are flatter than those of the loop libraries indicative of a more promiscuous activity. (B) Dependence of recovery on the number of adenine residues. An increasing number of adenine residues reduces the recovery ratios of variants, indicating that adenine is targeted nonspecifically. Interestingly, there are some variants in both DNA libraries that exhibit much lower recovery ratios compared to those of the rest of the population. This indicates that some specific sequence pattern is targeted. (C) Minimum free energy structures of two sensitive variants from the SRL DNA library as predicted by NUPACK.[33] These variants form secondary hairpins with small loops. The small loops closely resemble the sensitive ACG pattern identified in the DNA loop library.

(Figure 3A, middle). A histogram representation of the abundance ratio shows that the distribution of the error is symmetric (Figure 3A, bottom) and the kernel density estimate (blue) of the distribution estimated from the data traces a normal distribution (red) fairly well. The method therefore does not seem to introduce any systematic bias, but it introduces a certain amount of normally distributed random error.

Sequence Preference of Saporin. All variants were ranked according to the ratio of relative abundance in the library after a 30 min saporin treatment in comparison to a 0 min treatment from lowest to highest. We call this measure the recovery ratio of the variants. This ranking reflects the preference of saporin for all variants in the library. Figure 3B shows the top 100 most depleted variants and a sequence logo for the top 20 variants.[31] The complete preference distributions can be found in Supporting Data 1.

Although an enrichment of certain bases can be observed in the top 20 variants of all libraries (see sequence logos in Figure 3), only the N6 loop DNA library clearly shows a preferred pattern. Here, variants that contained the ACGN or AAGN sequence motif in a tetraloop (colored black in the last column) were highly depleted. The same pattern in a hexaloop was much less sensitive to depurination by saporin. This result indicates the specificity of saporin for DNA tetraloops that start with an ACG or AAG sequence. No patters were obvious in the other libraries.

Interestingly, the ACGAGA wild-type SRL sequence (RNA) in the randomized region is not efficiently targeted by saporin. It ranks 3284th of 4096 in replicate 1 and 3379th in replicate 2. Therefore, >80% of the other variants are depurinated more efficiently by saporin than the wild-type SRL sequence. This was already suspected from the initial experiments, because the SRL-mimic RNA was depurinated and cleaved far less efficiently than the randomized library. Thus, in contrast to ricin that was shown to specifically depurinate the native SRL sequence,[9,32] saporin depurinates nucleic acids with different sequence requirements.

During the depurination of ribosomes, RIPs need to interact with ribosomal proteins to gain access to the SRL.[5,6] Depurination of isolated nucleic acids as demonstrated in our experiments might thus yield different specificities, because only direct saporin−nucleic acid interactions are possible.

Search for Other Preferred Sequence Patterns. To find any potentially hidden patterns in the other libraries, we tried the following approaches. First, all pairwise base interactions were estimated for contributions to saporin specificity. Second, enrichment of longer (three- and four-nucleotide) patterns among the 100 most depurinated sequences was investigated.

On the basis of the work of Guenther et al.,[23] we constructed a linear regression model that considers the pairwise coupling of bases. The linear coefficients of the models allow us to deduce which pair of bases significantly affects saporin specificity as compared to complete interaction matrices that can be harder to interpret. These significant interactions and the predicted (model) versus experimental comparison of the recovery ratios are shown in Figure 4.

We observed that the pairwise models for the different libraries could explain ∼60% of the data set obtained for RNA, but only ∼50% for DNA. Therefore, these models are unable to fit the data well. A likely explanation is the promiscuous nature of the catalytic activity of saporin. As has been shown previously, saporin can target all adenine residues in a DNA version of the SRL (see Figure 2D). When the enzyme is active on any adenine residue, the pairwise coupling with other bases should have minor effects. Complicating the interpretation is the fact that multiple adenine bases might be present in a given variant. Once a variant containing multiple adenine bases is depurinated and cleaved, it is impossible to determine which

https://doi.org/10.1021/acschembio.2c00531
ACS Chem. Biol. 2022, 17, 2619−2630

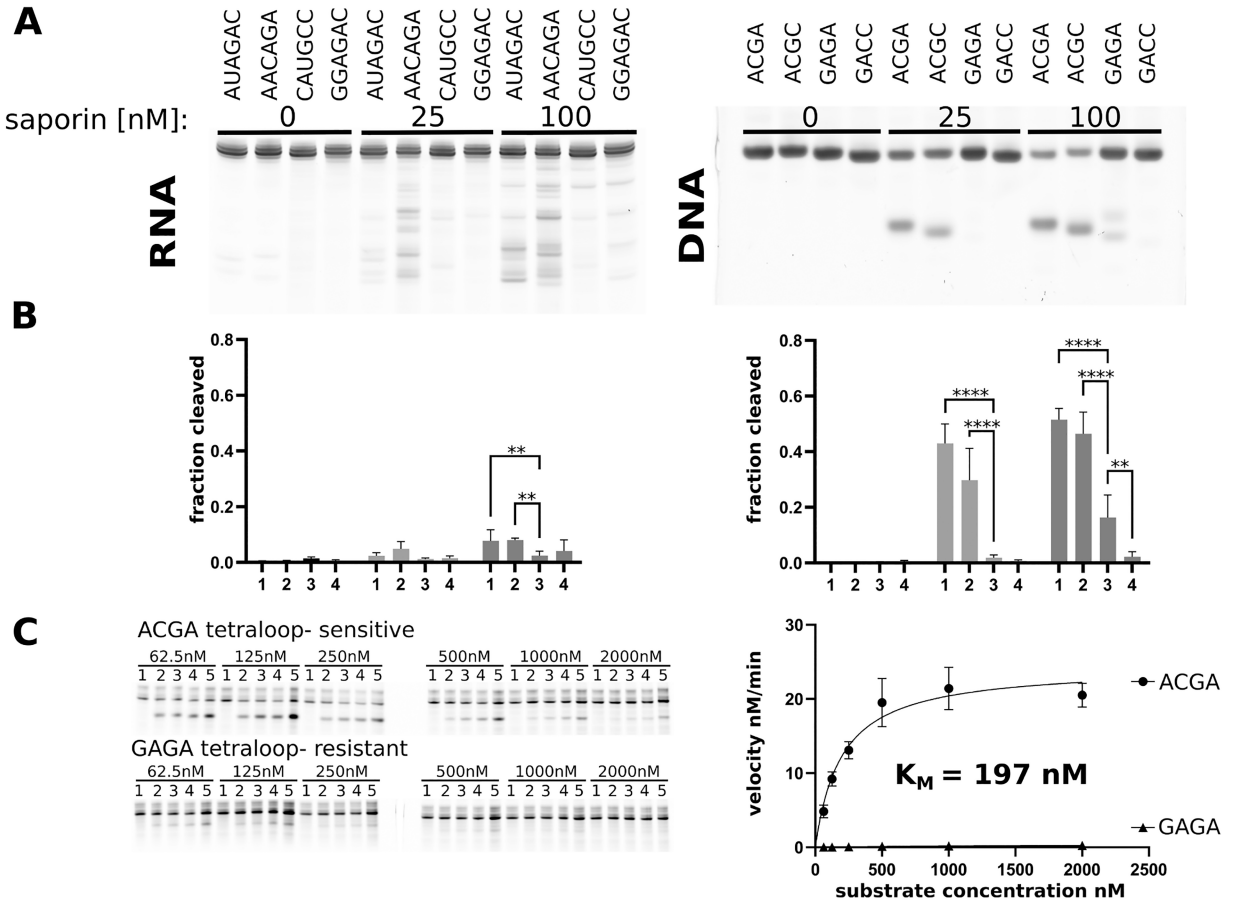

Figure 6. Confirmation of the sequencing results using PAGE. (A) Representative PAGE gels. RNA (500 nM) with randomized AUAGAC (lanes 1, 5, and 9), AACAGA (lanes 2, 6, and 10), CAUGCC (lanes 3, 7, and 11), and GGAGAC (lanes 4, 8, and 12) sequences were treated with the indicated amounts of saporin for 30 min at 37 °C before aniline treatment. DNA oligos OSaH455 (G-ACGA-C in lane lanes 1, 5, and 9), OSaH456 (G-ACGC-C in lanes 2, 6, and 10), OSaH457 (G-GAGA-C in lanes 3, 7, and 11), and OSaH458 (G-GACC-C in lanes 4, 8, and 12) at 500 nM were incubated with the indicated amounts of saporin for 30 min at 37 °C before aniline treatment. Only the sequence in the loop is shown in the figure. (B) Quantification of the fraction cleaved (FL) from PAGE gels using three separate experiments. Shown are the average and standard deviation. Asterisks indicate statistically significant differences at the $^{**}p < 0.01$ or $^{****}p < 0.0001$ level. (C) Kinetic analysis of the most sensitive ACGA tetraloop variant and a tetraloop variant containing the GAGA SRL motif. The indicated amounts of 5′FAM-labeled substrates OSaH525 and OSaH526 were incubated with 20 nM saporin at 37 °C. The gel pictures show cleavage after (1) 0, (2) 5, (3) 10, (4) 15, and (5) 30 min for the sensitive ACGA variant and (1) 0, (2) 30, (3) 50, (4) 90, and (5) 180 min for the GAGA tetraloop variant. Note that the contrast was adjusted in both pictures to better show the cleavage products. The experiment was repeated three times, and the initial reaction velocity estimated after 5 min for the ACGA variant and after 180 min for the GAGA variant. A plot of the average initial velocity against the substrate concentration is shown at the right. Error bars indicate the standard deviation from three experiments. Nonlinear regression was performed to estimate the K_M for the sensitive ACGA tetraloop.

position was targeted by saporin or if multiple positions were depurinated. Therefore, highly promiscuous activity cannot be captured accurately with this kind of model. Nevertheless, pairwise coupling of bases seems to determine the sequence preference of saporin for RNA to a higher degree than for DNA. Higher-order interactions than pairwise, for example, the previously observed ACG pattern in a tetraloop, could contribute more to how saporin discriminates DNA sequences.

Promiscuous Activity or Specificity? The data analyzed thus far suggest highly promiscuous activity of saporin while also showing specificity for certain DNA tetraloops. The data obtained by sequencing cover the complete sequence space, so it is possible to also inspect the overall distribution of recovery ratios. These distributions show that there is a clear difference between the libraries based on the SRL and the shorter loop libraries (see Figure 5A). The distributions of the SRL libraries are more spread out, indicating promiscuous activity across a broad range of variants, while distributions of the loop libraries are more compact, suggesting that saporin is less active on most variants.

The higher activity of saporin on SRL libraries might be caused by the additional adenine bases outside of the randomized region. Although it is not possible to determine which adenine in a specific sequence is targeted by saporin, it is possible to investigate the effect of the number of adenines in a specific sequence on its reactivity. Nonspecific activity of saporin toward adenine should result in an increased reactivity the more adenines are present in the sequence. The box plots shown in Figure 5B show an increasing degree of depurination as the number of adenines in a sequence increases. However, the trend is much less pronounced in the DNA tetraloop library. Other bases (C, G, and U/T) do not show similar trends (Figure S4).

https://doi.org/10.1021/acschembio.2c00531
ACS Chem. Biol. 2022, 17, 2619−2630

Other interesting features of the plots in Figure 5B are differences in the tails of the distributions. For the two RNA libraries, there are only a few variants in the tails of the distributions, while there are a significant number of variants with one or two adenines with very low recovery ratios in the DNA libraries. This suggests that these variants are targeted sequence specifically rather than nonspecifically by saporin.

As mentioned above, the variants with the lowest recovery ratios in the DNA loop library contain the ACG motif in a tetraloop. The predicted secondary structures of the highly depleted variants containing one or two adenines from the SRL-based library suggest that they may form smaller hairpins with a tetraloop resembling the ACG motif (Figure 5C).

Confirmation of Sequencing Results. Variants from the top, middle, and bottom of the preference distribution were selected and treated with saporin to confirm the different preferences inferred by sequencing. After saporin treatment, the oligos were cleaved by aniline and analyzed by PAGE. Variants from the loop libraries were selected because they exhibited the clearest preference patterns. According to the sequencing results for RNA, two variants sensitive to depurination by saporin (AUAGAC and AACAGA), one variant with intermediate sensitivity (CAUGCC), and one variant resistant to depurination (GGAGAC) were picked for analysis. Panels A and B of Figure 6 show the results for the RNA substrates. The bands corresponding to cleavage products are more intense for the sensitive variants than for the other two, indicating that these are indeed more readily depurinated by saporin.

From the DNA loop library, we also selected two sensitive variants (G-**ACGA**-C and G-**ACGC**-C), one intermediate variant (G-**GAGA**-C), and one resistant variant (G-**GACC**-C). All of these variants are predicted to form a tetraloop and contain at least one adenine base in the loop that could theoretically be targeted by saporin. Panels A and B of Figure 6 show that the variants that should be sensitive according to the sequencing results were efficiently cleaved even at low saporin concentrations. The oligo with the GAGA loop (intermediate sensitivity according to sequencing) showed visible cleavage only at the high saporin concentration, while the supposedly resistant GGACCC variant did not show clear cleavage bands. Treatment of these selected oligos with saporin thus yielded the cleavage band intensities expected from the sequencing results.

To further validate the results obtained by sequencing, the kinetics of cleavage of the most sensitive DNA variant containing the ACGA tetraloop was investigated. Varying concentrations of the tetraloop variant were reacted with 20 nM saporin for 5, 10, 15, or 30 min, and the amount of product produced was estimated by a PAGE assay. The oligo was fluorescently labeled with a FAM fluorophore at the 5′ end to facilitate quantification. From the initial reaction velocities, Michaelis constant K_M was estimated to be 197 nM [95% confidence interval (CI) from 133.2 to 287.6 nM] and v_{max} to be 24.3 nM/min (95% CI from 21.8 to 27.4 nM/min). We also tried to estimate the kinetic parameters for the GAGA tetraloop substrate that mimics the native SRL substrate. Cleavage of this substrate was too slow to accurately estimate the kinetic parameters using our assay (Figure 6C). Previous reports of K_M values for native substrates range from 9 to 95 μM.[29,30] Therefore, our sequencing assay identified DNA substrates with a higher affinity (lower K_M) for saporin compared to those of native SRL sequences.

DISCUSSION

The main findings of this study are (1) the wild-type SRL sequence is not efficiently targeted by saporin, (2) saporin depurinates all adenine residues in single-stranded regions of DNA at high saporin concentrations, and (3) saporin most efficiently targets DNA hairpins containing tetraloops starting with the bases ACG.

Although the SRL sequence is generally assumed to be the natural target of RIPs, most sequences in the randomized RNA library based on the SRL are depurinated more efficiently than the SRL. It has been suggested that for specific nucleic acid binding proteins the natural substrate sequences are located at the top of the affinity distribution while for nonspecific proteins the natural substrates are located in the middle of the distribution.[23] Using this interpretation would suggest that the RNA:adenosine glycosidase activity of saporin is nonspecific, because the natural SRL substrate is not preferentially depurinated, but located closer to the end of our preference distribution. In contrast to the nonspecific action toward RNA, we found that saporin preferentially targets DNA hairpins at a tetraloop containing the ACG sequence. This seems to be achieved by a higher affinity for variants containing a tetraloop with the ACGN motif.

Our sequencing assay provides information about the target specificity (or lack thereof) of saporin and other depurinating enzymes. However, there are several limitations that need to be considered. As presented, this assay is based on single-time-point measurements of the substrates reacted with saporin. Therefore, it can provide relative reactivities of the substrates only under a specific condition (reaction time, enzyme concentration, etc.), which significantly affects the outcome. A parallel assay of multiple time points should provide more information about the substrate specificity and kinetics at the cost of additional labor and sequencing capacity. Another limitation is that the assay provides no information about the site of reaction when there are multiple adenines in the substrate.

This is the first time that a highly specific DNA motif has been reported for a RIP. The result might encourage more investigations into the effect of RIPs on DNA. However, ssDNA and DNA hairpins occur rarely in living cells. Some examples where ssDNA occurs are during DNA replication,[34] DNA repair,[35] and transcription,[36] in R loops,[37] or in viral genomes and during their replication.[38] A feature of many RIP that is difficult to explain on the basis of their rRNA:adenosine glycosidase activity is their antiviral property.[39,40] More general RNA- and DNA-targeting activity could in part explain the observed antiviral effects. It also seems possible that some DNA viruses that infect *S. officinalis* could carry sequences that form hairpins with the recognition motif in the loop. The same could be true for other RIPs that have been suggested to protect plants from viruses.[41,42] RIPs could thus be part of the plant immune defenses to target and destroy foreign DNA (or RNA) sequences that contain the targeted motif.

In light of our results, saporin-based immunotoxins might also not primarily target protein synthesis, but act by attacking DNA. This can lead to side effects different from would be expected after ribosome inactivation. RIPs are also known to cause nuclear damage and apoptosis, but so far, no direct link between ribosome inactivation and apoptosis activation has been proven.[43,44] Preferential depurination of DNA over RNA could explain such observations. In this case, nucleus to

https://doi.org/10.1021/acschembio.2c00531
ACS Chem. Biol. 2022, 17, 2619−2630

Table 1. Sequences of Oligonucleotides Used

oligo	sequence (5′ to 3′)
OSaH151 (RNA)	GGGUGCUCAGUACGAGAGGAACCGCACCC
OSaH229 (RNA)	GGGAUGCUGCUCAGUACGAGAGGAACCGCAGCAUCCC
OSaH130	GTGACTGGAGTTCAGACGTG
OSaH152	GGGTGCTCAGTACGAGAGGAACCGCACCC
OSaH190	GGGATGCTGCTCAGTACGAGAGGAACCGCAGCATCCC
OSaH195	GGGATGCTGCTCAGTACGTGAGGAACCGCAGCATCCC
OSaH196	GGGATGCTGCTCAGTACGAGTGGAACCGCAGCATCCC
OSaH199	GGGATGCTGCTCTGTTCGTGTGGTTCCGCAGCATCCC
OSaH201	GGGATGCTGCTCAGTACGTGTGGAACCGCAGCATCCC
OSaH207	GGGATGCTGCTCTGTTCGAGTGGTTCCGCAGCATCCC
OSaH208	GGGATGCTGCTCTGTTCGTGAGGTTCCGCAGCATCCC
OSaH209	GGGATGCTGCTCTGTTCGAGAGGTTCCGCAGCATCCC
OSaH243	GGGATGCTGCTCTGTTCGTGTGGAACCGCAGCATCCC
OSaH244	GGGATGCTGCTCAGTACGTGTGGTTCCGCAGCATCCC
OSaH247	GTGACTGGAGTTCAGACGTGTGCTCTTCCGATCTTTATCCTCTAGCAGCAGGACGG
OSaH249	GTGACTGGAGTTCAGACGTGTGCTCTTCCGATCTTAGAGTAGACAAGCAGCAGGACGG
OSaH266	GCCTTCCTTCGTTCGGGTGCCGGCNNNNNNGCCGGTGCCCGTCCTGCTGCT
OSaH268	TAATACGACTCACTATAGGGCCTTCCTTCGTTCGGGTGC
OSaH269	AGCAGCAGGACGGGCACCG
OSaH337	GCCTTCCTTCGTTCGGGTGCCGGCGACGACGCCGGTGCCCGTCCTGCTGCT
OSaH378	GCCTTCCTTCGTTCGGGTGCCGGCTCAGTNNNNNNGGAACCGCCGGTGCCCGTCCTGCTGCT
OSaH382	ACACTCTTTCCCTACACGACGCTCTTCCGATCTGCCTTCCTTCGTTCGGGTGCCGGC
OSaH402	GCCTTCCTTCGTTCGGGTGCCGGCtcagtACGAGAggaaccGCCGGTGCCCGTCCTGCTGCT
OSaH455	CGGGTGCCGGCGACGACGCCGGTGCCCG
OSaH456	CGGGTGCCGGCGACGCCGCCGGTGCCCG
OSaH457	CGGGTGCCGGCGGAGACGCCGGTGCCCG
OSaH458	CGGGTGCCGGCGGACCCGCCGGTGCCCG
OSaH466	GCCTTCCTTCGTTCGGGTGCCGGCATAGACGCCGGTGCCCGTCCTGCTGCT
OSaH467	GCCTTCCTTCGTTCGGGTGCCGGCAACAGAGCCGGTGCCCGTCCTGCTGCT
OSaH468	GCCTTCCTTCGTTCGGGTGCCGGCCATGCCGCCGGTGCCCGTCCTGCTGCT
OSaH469	GCCTTCCTTCGTTCGGGTGCCGGCGGAGACGCCGGTGCCCGTCCTGCTGCT
OSaH517	GGGTGCTCAGTACGAGAGGAACCCGCCAC
OSaH518	GTGGCGTCAGTACGAGAGGAACCGCACCC
OSaH519	GCCTTCCTTCGTTCGGGTGCCGGCTCAGTACGAGAGGAACCGGTCCGCGCCGTCCTGCTGCT
OSaH520	GCCTTCCTTCGTTCGGCGCGGAGGTCAGTACGAGAGGAACCGCCGGTGCCCGTCCTGCTGCT
OSaH521	GCCTTCCTTCGTTCGGGTGCCGGCCGAGAGGGTCCGCGCCGTCCTGCTGCT
OSaH522	GCCTTCCTTCGTTCGGCGCGGAGGCGAGAGGCCGGTGCCCGTCCTGCTGCT
OSaH523	GGGATGCTGCTCAGTACGAGAGGAACCGCCAGCACCT
OSaH524	AGGTGCTGGCTCAGTACGAGAGGAACCGCAGCATCCC
OSaH525	FAM-CGGGTGCCGGCGACGACGCCGGTGCCCG
OSaH526	FAM-CGGGTGCCGGCGGAGACGCCGGTGCCCG

mitochondria (NM) signaling[45] might be the missing link between RIP activity and apoptosis. Some RIPs have even been shown to enter the nucleus and enrich the nucleoli,[46,47] a place with strong transcriptional activity where ssDNA segments might be present.

Finally, a more general observation is that the most sensitive variants of the DNA libraries were depurinated more than the most sensitive RNA variants (recovery ratios of >70% for RNA and <40% for DNA). Interestingly, other RIPs also preferentially target DNA over RNA,[10,28] so the DNA:adenosine glycosidase activity may be a general feature of RIPs that has not received sufficient attention. Using our method, it is now possible to study the sequence preference of other RIPs, including important toxins such as ricin and Shiga toxin. It is also possible to sequence samples from multiple time points to obtain detailed kinetic data on the depurination of all variants in the library similar to the results obtained for C5.[23]

MATERIALS AND METHODS

Oligonucleotides. All oligonucleotides used in this study were ordered from Eurofins Genomics, IDT, or Sigma and are summarized in Table 1. The oligos were stored as 100 μM stocks in water. Before use in depurination assays, the oligos were diluted to 2 or 20 μM in water, heated for 3 min at 98 °C and rapidly cooled on ice. These stocks were stored at −20 °C until use.

In Vitro Transcription. Primers OSaH268 and OSaH269 were used to amplify constructs of randomized oligos OSaH378 and OSaH266 (33 nM) containing the T7 promoter. Q5 High-Fidelity 2X Master Mix [New England Biolabs (NEB)] was used for PCR with 33 nM template and 1.6 μM primers in 60 μL reaction mixtures. The thermal cycling conditions for all PCRs can be found in the Supporting Information.

The dsDNA products were purified from a 2.5% agarose gel (25 min at 135 V, stained with ethidium bromide) using the Zymoclean Gel DNA Recovery Kit (Zymo Research) with two additional washing steps to ensure complete removal of agarose. The libraries were eluted with 16 μL of water, and the concentration was measured using NanoDrop One (Thermo Fisher). RNA was transcribed from

https://doi.org/10.1021/acschembio.2c00531
ACS Chem. Biol. 2022, 17, 2619−2630

DNA templates using T7 RNA polymerase (NEB) according to the manufacturer's instructions for 12−16 h. After digestion of the DNA template for 30 min at 37 °C with DNaseI (Takara Bio), RNA was purified using the RNA Clean and Concentrator-5 Kit (Zymo Research). The RNA concentration was determined using NanoDrop One.

For the confirmation of the sequencing results, DNA templates were generated as described above using oligo OSaH466, OSaH467, OSaH468, or OSaH469 as the template. The DNA was purified using the DNA Clean and Concentrator-5 Kit (Zymo Research). RNA was transcribed as described above and PAGE purified after DNase I digestion.

PAGE. Polyacrylamide gels were cast using a premixed 40% acrylamide/bisacrylamide solution at the final concentrations indicated with 7 M urea. Gels were run at 200 V for 60 min (8%) or 100 min (16%). RNA and DNA were stained in polyacrylamide gels in 40 mL of TBE with 1× SYBR Gold for 10 min and then visualized using a GE Typhoon FLA 9000 scanner.

For PAGE purification, the bands of interest were cut from the gel, finely crushed inside a microcentrifuge tube, and extracted with 300 μL of extraction buffer [30 mM Tris (pH 7.5) and 30 mM NaCl] at 4 °C overnight. The gel was then pelleted at 21000*g* for 2 min, and the supernatant was carefully removed. Nucleic acids were recovered from the supernatant by ethanol precipitation [with 0.1 volume of 3 M sodium acetate (pH 5.2) and 3 volumes of 99% ethanol] and dissolved in water at the volume required for further processing.

Saporin Treatment and Aniline Cleavage. Saporin treatment and aniline cleavage were performed according to a previous report.[3] Briefly, DNA oligos or in vitro-transcribed RNA was incubated with the indicated amounts of saporin (S9896, Sigma-Aldrich) in 30 μL of reaction buffer [25 mM Tris (pH 7.5), 25 mM KCl, and 5 mM $MgCl_2$] at 37 °C for 30 min or as long as indicated. The reactions were quenched by adding SDS to a final concentration of 2% from a 10% stock solution. After saporin treatment, the oligos were precipitated by addition of 0.1 volume of 3 M sodium acetate and 3 volumes of 99% ethanol with centrifugation at 18000*g* and 4 °C for 15 min. The pellets were resuspended in 20 μL of acetic acid/aniline (2.5 and 1 M) and incubated at 60 °C for 5 min. Aniline was removed by extraction with 500 μL of diethyl ether and acetic acid by an additional round of ethanol precipitation. Finally, the pellets were resuspended in 3 μL of water and 3 μL of 2× RNA loading buffer for PAGE analysis or purification. For the confirmation experiment with RNA, the reaction was scaled down using half of the amounts of all components.

Reverse Transcription. For reverse transcription, a mixture of saporin-treated RNA (3 μL), reverse transcription primer (1.5 μL, 10 μM), 2.5 mM dNTPs (2.5 μL), and water (0.5 μL) was denatured at 98 °C for 3 min and cooled to 4 °C. Then, 5× buffer (2 μL), RNase inhibitor, murine (0.25 μL, NEB), and Maxima H Minus Reverse Transcriptase (0.25 μL, Thermo Fisher) were added. The reaction mixture was incubated at 50 °C for 30 min and then at 85 °C for 5 min. The cDNA was separated and purified on a denaturing polyacrylamide gel (8%). The reverse transcription primers were OSaH247 and OSaH249. These contained different barcodes for different treatment times (0 and 30 min, respectively).

The second strand of cDNA was synthesized in a PCR using NEB Q5Mastermix and primers OSaH130 and OSaH382 (final concentration of 50 nM) with 2 μL of the cDNA (resuspended in 10 μL of water after gel extraction) as the template in a total volume of 20 μL. In the case of DNA oligos, OSaH382 and OSaH247 or OSaH249 were used in the first PCR (also using 2 μL of a saporin-treated library recovered by PAGE and resuspended in 10 μL of water) to add the sequencing adapters.

Preparation of the Sequencing Library. A second PCR using Illumina UDI primers was performed using 1.5 μL of the first PCR as the template. This PCR was performed twice. First, 5 μL of PCR mix was loaded on a 3% agarose gel after 5, 10, and 15 cycles to estimate the number of cycles necessary to obtain a sufficient amount of the final library. The gels were stained using ethidium bromide, and the amounts of the products were estimated by comparison with the band intensity of the DNA size marker (50 bp DNA ladder, NEB). The second repeat of this PCR was performed for the number of cycles judged necessary (five to eight cycles) using 30 μL reaction mixtures. After the addition of 6× loading dye, the complete PCR mix was loaded into two wells of a 3% agarose gel, run for 25 min at 135 V, stained with ethidium bromide, and cut from the gel. The DNA was recovered using the gel extraction kit with two additional washing steps to ensure complete removal of agarose. The libraries were eluted with 8 μL of water, and the concentration was measured using NanoDrop One.

Sequencing and Data Analysis. Sequencing was performed using Illumina NovaSeq by OIST DNA Sequencing Section. The reads corresponding to different treatment times were selected on the basis of the barcode added during the first PCR or reverse transcription. From these reads, the randomized section was extracted and the occurrence of each sequence was counted using a bash script.

From the raw sequencing count for each variant, the relative abundance in the library was calculated by division by the sum of the count of all variants in the respective library. The recovery ratio of each library was then calculated by dividing the relative abundance after treatment and the relative abundance before treatment. This measure was used to rank variants from sensitive (low recovery ratio) to resistant (high recovery ratio). To quantify the cleavage rate for different variants from PAGE data, the average intensities of the cleaved and uncleaved bands were measured using ImageJ. The fraction cleaved (FL) was calculated by dividing the intensity of the cleaved bands by the sum of the intensities of the cleaved and uncleaved bands after subtracting the gel background and normalizing for the measured area. Three independent experiments were performed, and statistically significant differences determined using a two-way analysis of variance (ANOVA) in GraphPad Prism 9 with the FDR method of Benjamini and Hochberg.

Native PAGE. Each oligo (500 nM) was incubated in 10 μL of reaction buffer [25 mM Tris (pH 7.5), 25 mM KCl, and 5 mM $MgCl_2$] at 98 °C for 3 min and then immediately cooled on ice. Slow cooling was performed in a Bio-Rad T100 cycler at 0.1 °C/s until 4 °C was reached. Samples were then mixed with an equal volume of loading dye (2× TBE, 50% glycerol, and 0.1% bromophenol blue), loaded onto a 15% native polyacrylamide gel, and run at 200 V for 60 min, before being stained with SYBR Gold. Imaging was performed with a GE Typhoon FLA 9500 imager.

Kinetic Analysis. For kinetic analysis, different concentrations of 5′FAM-labeled oligos OSaH525 and OSaH526 were incubated with 20 nM saporin in 40 μL of reaction buffer at 37 °C (heat block) for the indicated times. At each time point, the reaction was quenched by addition of SDS to a final concentration of 2%. The samples were precipitated with ethanol and sodium acetate, treated with aniline, washed with ether, and precipitated again, as described in Saporin Treatment and Aniline Cleavage. In each lane of a 16% denaturing urea−polyacrylamide gel was loaded 2.5 pmol of the oligo, and the gel was run at 200 V for 60 min. The gels were imaged using a GE Typhoon FLA 9500 instrument, and the bands corresponding to full length and cleaved oligos were quantified with ImageJ. The fraction cleaved was calculated as described above. This was multiplied by the initial substrate concentration to estimate the product concentration at each time point. For the sensitive substrate, the initial reaction velocity was estimated using the product concentration at 5 min, and at 180 min for the resistant oligo. The experiments were performed three times independently. A nonlinear fit to the Michaelis−Menten equation was performed using GraphPad Prism 9 to estimate the kinetic parameters.

Pairwise Coupling Model. We used a model similar to that of Guenther et al.[23] The model consists of position terms x that are described by the linear coefficients β. x is equal to 1 if there is a specific base at a specific position or 0 otherwise. N equals 24 for four nucleotides at six positions.

$$\text{recovery ratio} = \beta_0 + \sum_{i=1}^{N} \beta_i x_i$$

https://doi.org/10.1021/acschembio.2c00531
ACS Chem. Biol. 2022, 17, 2619−2630

Next, pairwise terms were created, where each variable is 0 or 1 if the sequence has a pair of nucleotides in specific positions (e.g., A3U6). This creates a total of 240 pairwise terms. The position model presented above was then fitted with a separate pairwise term 240 times using the ordinary least-squares linear regression model from the Statmodels Python package. The pairwise terms with a p value of <0.000005, indicating linear coefficients not statistically higher than zero, were discarded. Next, all statistically significant terms were added to the position model. The model was then trimmed with stepwise regression. We used backward elimination, where starting from the full set of variables, the model was iteratively fitted as described above, but at each iteration, the least statistically significant term (highest p value) was removed until all terms were significant. This led to a position model with significant pairwise terms added. The model was then used to predict the values of all variables. The R^2 score (coefficient of determination) between predicted and observed values was calculated using the r2_score function from the Python scikit-learn package.

■ ASSOCIATED CONTENT

Supporting Information

The Supporting Information is available free of charge at https://pubs.acs.org/doi/10.1021/acschembio.2c00531.

PCR protocols, native PAGE experiments that confirm the oligos used do not form duplexes, control experiments for the nonspecific depurination of DNA oligos, linear correlations between two replicates for all libraries and conditions, correlations of the recovery ratio to the number of each nucleotide base, and a picture of the second replicate of the PAGE gel shown in Figure 1 (PDF)

Spreadsheet containing raw sequencing counts for all variants in each library as well as the derived recovery ratio (data1) (XLSX)

Spreadsheet containing the number of occurrences of each 3- and 4-base pattern among the 100 variants with the lowest recovery ratio (data2) (XLSX)

■ AUTHOR INFORMATION

Corresponding Author

Yohei Yokobayashi − *Nucleic Acid Chemistry and Engineering Unit, Okinawa Institute of Science and Technology Graduate University, Onna, Okinawa 904-0495, Japan;* orcid.org/0000-0002-2417-1934; Email: yohei.yokobayashi@oist.jp

Authors

Samuel Hauf − *Nucleic Acid Chemistry and Engineering Unit, Okinawa Institute of Science and Technology Graduate University, Onna, Okinawa 904-0495, Japan;* orcid.org/0000-0002-3034-8441

Rachapun Rotrattanadumrong − *Nucleic Acid Chemistry and Engineering Unit, Okinawa Institute of Science and Technology Graduate University, Onna, Okinawa 904-0495, Japan*

Complete contact information is available at: https://pubs.acs.org/10.1021/acschembio.2c00531

Notes

The authors declare no competing financial interest.

■ ACKNOWLEDGMENTS

This work was funded by the Deutsche Forschungsgemeinschaft (DFG, Project number 452628014, Geschäftszeichen HA9374/1-1 to S.H.) and funds from the Okinawa Institute of Science and Technology Graduate University. R.R. was supported by the Research Fellowship for Young Scientists (DC2) and KAKENHI (21J10391) from the Japan Society for the Promotion of Science (JSPS). The authors thank the OIST DNA Sequencing Section for sequencing support and the Scientific Computing and Data Analysis section of the Research Support Division at OIST for the help and support provided.

■ REFERENCES

(1) Schrot, J.; Weng, A.; Melzig, M. F. Ribosome-inactivating and related proteins. *Toxins (Basel).* **2015**, *7*, 1556−1615.

(2) Voorhees, R. M.; Schmeing, T. M.; Kelley, A. C.; Ramakrishnan, V. The mechanism for activation of GTP hydrolysis on the ribosome. *Science.* **2010**, *330*, 835−838.

(3) Endo, Y.; Mitsui, K.; Motizuki, M.; Tsurugi, K. The mechanism of action of ricin and related toxic lectins on eukaryotic ribosomes. The site and the characteristics of the modification in 28 S ribosomal RNA caused by the toxins. *J. Biol. Chem.* **1987**, *262*, 5908−5912.

(4) Montanaro, L.; Sperti, S.; Mattioli, A.; Testoni, G.; Stirpe, F. Inhibition by ricin of protein synthesis in vitro. Inhibition of the binding of elongation factor 2 and of adenosine diphosphate-ribosylated elongation factor 2 to ribosomes. *Biochem. J.* **1975**, *146*, 127−131.

(5) Li, X.-P.; Kahn, J. N.; Tumer, N. E. Peptide Mimics of the Ribosomal P Stalk Inhibit the Activity of Ricin A Chain by Preventing Ribosome Binding. *Toxins (Basel).* **2018**, *10*, 371.

(6) Rudolph, M. J.; Davis, S. A.; Tumer, N. E.; Li, X.-P. Structural basis for the interaction of Shiga toxin 2a with a C-terminal peptide of ribosomal P stalk proteins. *J. Biol. Chem.* **2020**, *295*, 15588−15596.

(7) Endo, Y.; Tsurugi, K. The RNA N-glycosidase activity of ricin A-chain. The characteristics of the enzymatic activity of ricin A-chain with ribosomes and with rRNA. *J. Biol. Chem.* **1988**, *263*, 8735−8739.

(8) Olsnes, S.; Fernandez-Puentes, C.; Carrasco, L.; Vazquez, D. Ribosome inactivation by the toxic lectins abrin and ricin. Kinetics of the enzymic activity of the toxin A-chains. *Eur. J. Biochem.* **1975**, *60*, 281−288.

(9) Glück, A.; Endo, Y.; Wool, I. G. Ribosomal RNA identity elements for ricin A-chain recognition and catalysis. Analysis with tetraloop mutants. *J. Mol. Biol.* **1992**, *226*, 411−424.

(10) Amukele, T. K.; Roday, S.; Schramm, V. L. Ricin A-chain activity on stem-loop and unstructured DNA substrates. *Biochemistry.* **2005**, *44*, 4416−4425.

(11) Barbieri, L.; Valbonesi, P.; Bonora, E.; Gorini, P.; Bolognesi, A.; Stirpe, F. Polynucleotide:adenosine glycosidase activity of ribosome-inactivating proteins: effect on DNA, RNA and poly(A). *Nucleic Acids Res.* **1997**, *25*, 518−522.

(12) Barbieri, L.; Valbonesi, P.; Gorini, P.; Pession, A.; Stirpe, F. Polynucleotide: adenosine glycosidase activity of saporin-L1: effect on DNA, RNA and poly(A). *Biochem. J.* **1996**, *319*, 507−513.

(13) Barbieri, L.; Polito, L.; Bolognesi, A.; Ciani, M.; Pelosi, E.; Farini, V.; Jha, A. K.; Sharma, N.; Vivanco, J. M.; Chambery, A.; Parente, A.; Stirpe, F. Ribosome-inactivating proteins in edible plants and purification and characterization of a new ribosome-inactivating protein from Cucurbita moschata. *Biochim. Biophys. Acta, Gen. Subj.* **2006**, *1760*, 783−792.

(14) Chan, Y. S.; Ng, T. B. Shiga toxins: from structure and mechanism to applications. *Appl. Microbiol. Biotechnol.* **2016**, *100*, 1597−1610.

(15) Waddell, T.; Cohen, A.; Lingwood, C. A. Induction of verotoxin sensitivity in receptor-deficient cell lines using the receptor glycolipid globotriosylceramide. *Proc. Natl. Acad. Sci. U. S. A.* **1990**, *87*, 7898−7901.

(16) Flavell, D. J.; Flavell, S. U.; Boehm, D. A.; Emery, L.; Noss, A.; Ling, N. R.; Richardson, P. R.; Hardie, D.; Wright, D. H. Preclinical studies with the anti-CD19-saporin immunotoxin BU12-SAPORIN for the treatment of human-B-cell tumours. *Br. J. Cancer* **1995**, *72*, 1373−1379.

(17) Flavell, D. J.; Boehm, D. A.; Noss, A.; Warnes, S. L.; Flavell, S. U. Therapy of human T-cell acute lymphoblastic leukaemia with a combination of anti-CD7 and anti-CD38-SAPORIN immunotoxins is significantly better than therapy with each individual immunotoxin. *Br J. Cancer.* **2001**, *84*, 571−578.
(18) Shen, Q.; Xu, L.; Li, R.; Wu, G.; Li, S.; Saw, P. E.; Zhou, Y.; Xu, X. A tumor microenvironment (TME)-responsive nanoplatform for systemic saporin delivery and effective breast cancer therapy. *Chem. Commun. (Camb).* **2021**, *57*, 2563−2566.
(19) Castiello, M. C.; et al. Efficacy and safety of anti-CD45-saporin as conditioning agent for RAG deficiency. *J. Allergy Clin. Immunol.* **2021**, *147*, 309−320.e6.
(20) Wenk, G. L.; Stoehr, J. D.; Quintana, G.; Mobley, S.; Wiley, R. G. Behavioral, biochemical, histological, and electrophysiological effects of 192 IgG-saporin injections into the basal forebrain of rats. *J. Neurosci.* **1994**, *14*, 5986−5995.
(21) Cutuli, D.; Landolfo, E.; Nobili, A.; de Bartolo, P.; Sacchetti, S.; Chirico, D.; Marini, F.; Pieroni, L.; Ronci, M.; D'Amelio, M.; D'Amato, F. R.; Farioli-Vecchioli, S.; Petrosini, L. Behavioral, neuromorphological, and neurobiochemical effects induced by omega-3 fatty acids following basal forebrain cholinergic depletion in aged mice. *Alzheimer's Res. Ther.* **2020**, *12*, 150.
(22) Vallera, D. A.; Kreitman, R. J. Immunotoxins Targeting B cell Malignancy—Progress and Problems With Immunogenicity. *Biomedicines.* **2019**, *7*, 1.
(23) Guenther, U.-P.; Yandek, L. E.; Niland, C. N.; Campbell, F. E.; Anderson, D.; Anderson, V. E.; Harris, M. E.; Jankowsky, E. Hidden specificity in an apparently nonspecific RNA-binding protein. *Nature.* **2013**, *502*, 385−388.
(24) Jankowsky, E.; Harris, M. E. Specificity and nonspecificity in RNA-protein interactions. *Nat. Rev. Mol. Cell Biol.* **2015**, *16*, 533−544.
(25) Szewczak, A. A.; Moore, P. B. The sarcin/ricin loop, a modular RNA. *J. Mol. Biol.* **1995**, *247*, 81−98.
(26) Küpfer, P. A.; Leumann, C. J. The chemical stability of abasic RNA compared to abasic DNA. *Nucleic Acids Res.* **2007**, *35*, 58−68.
(27) Kivioja, T.; Vähärautio, A.; Karlsson, K.; Bonke, M.; Enge, M.; Linnarsson, S.; Taipale, J. Counting absolute numbers of molecules using unique molecular identifiers. *Nat. Methods.* **2012**, *9*, 72−74.
(28) Brigotti, M.; Carnicelli, D.; Vara, A. G. Shiga toxin 1 acting on DNA in vitro is a heat-stable enzyme not requiring proteolytic activation. *Biochimie.* **2004**, *86*, 305−309.
(29) Tang, S.; Hu, R. G.; Liu, W. Y.; Ruan, K. C. Non-specific depurination activity of saporin-S6, a ribosome-inactivating protein, under acidic conditions. *Biol. Chem.* **2000**, *381*, 769−772.
(30) Sturm, M. B.; Tyler, P. C.; Evans, G. B.; Schramm, V. L. Transition state analogues rescue ribosomes from saporin-L1 ribosome inactivating protein. *Biochemistry.* **2009**, *48*, 9941−9948.
(31) Crooks, G. E.; Hon, G.; Chandonia, J. M.; Brenner, S. E. WebLogo: A sequence logo generator. *Genome Res.* **2004**, *14*, 1188−1190.
(32) Endo, Y.; Glück, A.; Wool, I. G. Ribosomal RNA identity elements for ricin A-chain recognition and catalysis. *J. Mol. Biol.* **1991**, *221*, 193−207.
(33) Zadeh, J. N.; Steenberg, C. D.; Bois, J. S.; Wolfe, B. R.; Pierce, M. B.; Khan, A. R.; Dirks, R. M.; Pierce, N. A. NUPACK: analysis and design of nucleic acid systems. *J. Comput. Chem.* **2011**, *32*, 170−173.
(34) Nedelcheva-Veleva, M. N.; Krastev, D. B.; Stoynov, S. S. Coordination of DNA synthesis and replicative unwinding by the S-phase checkpoint pathways. *Nucleic Acids Res.* **2006**, *34*, 4138−4146.
(35) Sancar, A.; Lindsey-Boltz, L. A.; Unsal-Kaçmaz, K.; Linn, S. Molecular mechanisms of mammalian DNA repair and the DNA damage checkpoints. *Annu. Rev. Biochem.* **2004**, *73*, 39−85.
(36) Gaillard, H.; Aguilera, A. Transcription as a Threat to Genome Integrity. *Annu. Rev. Biochem.* **2016**, *85*, 291−317.
(37) Crossley, M. P.; Bocek, M.; Cimprich, K. A. R-Loops as Cellular Regulators and Genomic Threats. *Mol. Cell* **2019**, *73*, 398−411.
(38) Koonin, E. V.; Dolja, V. V.; Krupovic, M.; Varsani, A.; Wolf, Y. I.; Yutin, N.; Zerbini, F. M.; Kuhn, J. H. Global Organization and Proposed Megataxonomy of the Virus World. *Microbiol. Mol. Biol. Rev.* **2020**, *84*, e00061−19.
(39) Parikh, B. A.; Tumer, N. E. Antiviral activity of ribosome inactivating proteins in medicine. *Mini Rev. Med. Chem.* **2004**, *4*, 523−543.
(40) Stirpe, F.; Battelli, M. G. Ribosome-inactivating proteins: progress and problems. *Cell. Mol. Life Sci.* **2006**, *63*, 1850−1866.
(41) Di, R.; Tumer, N. E. Pokeweed Antiviral Protein: Its Cytotoxicity Mechanism and Applications in Plant Disease Resistance. *Toxins (Basel).* **2015**, *7*, 755−772.
(42) Wang, P.; Turner, N. E. Virus resistance mediated by ribosome inactivating proteins. *Adv. Virus Res.* **2000**, *55*, 325−355.
(43) Brigotti, M.; Alfieri, R.; Sestili, P.; Bonelli, M.; Petronini, P. G.; Guidarelli, A.; Barbieri, L.; Stirpe, F.; Sperti, S. Damage to nuclear DNA induced by Shiga toxin 1 and ricin in human endothelial cells. *FASEB J.* **2002**, *16*, 365−372.
(44) Das, M. K.; Sharma, R. S.; Mishra, V. Induction of apoptosis by ribosome inactivating proteins: importance of N-glycosidase activity. *Appl. Biochem. Biotechnol.* **2012**, *166*, 1552−1561.
(45) Fang, E. F.; Scheibye-Knudsen, M.; Chua, K. F.; Mattson, M. P.; Croteau, D. L.; Bohr, V. A. Nuclear DNA damage signalling to mitochondria in ageing. *Nat. Rev. Mol. Cell Biol.* **2016**, *17*, 308−312.
(46) Baibakov, B.; Murtazina, R.; Elowsky, C.; Giardiello, F. M.; Kovbasnjuk, O. Shiga toxin is transported into the nucleoli of intestinal epithelial cells via a carrier-dependent process. *Appl. Biochem. Biotechnol.* **2010**, *2*, 1318−1335.
(47) Vater, C. A.; Bartle, L. M.; Leszyk, J. D.; Lambert, J. M.; Goldmacher, V. S. Ricin A chain can be chemically cross-linked to the mammalian ribosomal proteins L9 and L10e. *J. Biol. Chem.* **1995**, *270*, 12933−12940.

https://doi.org/10.1021/acschembio.2c00531
ACS Chem. Biol. 2022, 17, 2619−2630